A peer-reviewed version of this preprint was published in PeerJ on 3 July 2014.

View the peer-reviewed version (peerj.com/articles/458), which is the preferred citable publication unless you specifically need to cite this preprint.

Hofmann R, Sander PM. 2014. The first juvenile specimens of *Plateosaurus engelhardti* from Frick, Switzerland: isolated neural arches and their implications for developmental plasticity in a basal sauropodomorph. PeerJ 2:e458 https://doi.org/10.7717/peerj.458

The first juvenile specimens of *Plateosaurus engelhardti* from Frick, Switzerland: Isolated neural arches and their implications for developmental plasticity in a basal sauropodomorph

Abstract

The dinosaur *Plateosaurus engelhardti* is the most abundant dinosaur in the Late Triassic of Europe and the best known basal sauropodomorph. *Plateosaurus engelhardti* was one of the first sauropdomorph dinosaurs to display a large body size. Remains can be found in the Norian stage of the Late Triassic in over 40 localities in Central Europe (France, Germany, Greenland and Switzerland). Since the first discovery of *P. engelhardti* no juvenile specimens of this species had been found. Here we describe the first remains of juvenile individuals, isolated cervical and dorsal neural arches. These were separated postmortem from their respective centra because of unfused neurocentral sutures. However the specimens share the same neural arch morphology found in adults. Morphometric analysis suggests a body lengths of the juvenile indivduals that is greater than those of most adult specimens. This supports the hypothesis of developmental plasticity in *Plateosaurus engelhardti* that previously had been based on histological data only. Alternative hypotheses for explaining the poor correlation between ontogenetic stage and size in this taxon are multiple species or sexual morphs with little morphological variance or time-averaging of individuals from populations differing in body size.

Keywords: Late Triassic, Norian, Switzerland, Basal Sauropodomorpha, *Plateosaurus engelhardti*, juvenile, neurocentral suture closure, bone histology.

Rebecca Hofmann (corresponding author), Division of Paleontology, Steinmann Institute, University Bonn, Nussallee 8, 53113 Bonn, Germany, Phone: 01635588589, [rebecca_hofmann@ymail.com]

P. Martin Sander, Division of Paleontology, Steinmann Institute, University Bonn, Nussallee 8, 53113 Bonn, Germany

Introduction

The prosauropods are a presumably paraphyletic assemblage of basal sauropodomorpha and form successive sistergroups to the largest terrestrial animals ever known, the Sauropoda, with which they form the Sauropodomorpha (Huene, 1932). Prosauropods were the dominant high-browsing herbivores from the late Norian until the end of the Early Jurassic, when they were replaced in dominance by sauropods (Barrett & Upchurch, 2005). The prosauropod *Plateosaurus* was one of the first larger-bodied dinosaurs. The first fossil remains of this taxon were found in 1834 at the Heroldsberg near Nuremberg by Johann Friedrich Philipp Engelhardt. The first to describe the material was Herman von Meyer in 1837 naming it *Plateosaurus engelhardti* (Moser, 2003).

Basal sauropodomorpha are important for understanding the unique gigantism of sauropod dinosaurs (Sander & Klein, 2005; Upchurch, Barrett & Galton, 2007) because they inform us about the plesiomorphic condition from which sauropod gigantism evolved. One such plesiomorphic condition may be the developmental plasticity seemingly present in *Plateosaurus engelhardti*, expressed in a poor correlation of ontogenetic stage and size (Sander & Klein, 2005). Developmental plasticity was initially hypothesized based on long bone histology (Sander & Klein, 2005), but in this paper we corroborate its presence based on body size at neurocentral suture closure, as documented by the first juvenile remains of *P. engelhardti*.

Systematics of *Plateosaurus*

A premise of any hypothesis of developmental plasticity is that the sample in question is derived from a single species. This necessitates a review of the systematics of *Plateosaurus*. The remains of *Plateosaurus* occur in the middle to the late Norian of Germany (Huene, 1926; Huene, 1932; Galton, 2001), France (Weishampel, 1984), Switzerland (Sander, 1992),

PeerJ PrePrints | http://dx.doi.org/10.7287/peerj.preprints.325v1 | CC-BY 4.0 Open Access | received: 30 Mar 2014, published: 30 Mar 2014

and Greenland (Jenkins et al., 1994). The type species of *Plateosaurus* is *P. engelhardti* Meyer, 1837. Several more species have been described from other localities in Germany such as *P. trossingensis* (Fraas, 1913) from Trossingen and *P. longiceps* (Jaekel, 1914a) from Halberstadt, and *P. gracilis* (Yates, 2003) from the Löwenstein Formation of Stuttgart. Currently the *Plateosaurus* finds from Halberstadt, Trossingen and Frick are currently assigned to one species: *P. engelhardti*. However, nomenclatorial controversy still surrounds this name (Galton, 1984a; Galton 1984b; Galton, 1985a; Galton, 1985b; Galton & Bakker, 1985; Weishampel & Chapman, 1990; Galton, 1997; Galton, 1999; Galton, 2000; Galton, 2001; Moser, 2003; Yates, 2003; Galton, 2012).

A massive abundance of *Plateosaurus* material found in "Plateosaurus bonebeds" (Sander, 1992) can be found at three localities: Halberstadt (Central Germany), Trossingen (Southern Germany) and Frick (Switzerland). The locality in Switzerland with a massive abundance of *Plateosaurus* material found in "Plateosaurus bonebeds" (Sander, 1992) is in an active clay quarry of the Keller AG in Frick (Canton Aargau, Switzerland), where the first dinosaurs fossils were discovered in 1963.

Plateosaurus from Frick: Geologic setting

Since the focus of this study lies on recently discovered juvenile *Plateosaurus* material, a review of this and other *Plateosaurus* bonebeds is necessary. The Gruhalde quarry exposes a section representing 20 million years of geologic time, from the entire Middle Keuper (Upper Triassic) up to the upper Sinemurian Obtusus clays (Early Jurassic) (Sander, 1990). The middle Keuper sediments are about 20 m thick, the upper 19 m of this section are the Upper Variegated Marls (Rieber, 1985; Sander, 1992). *Plateosaurus* remains are embedded in the Upper Variegated Marls (Norian), which is partially equivalent in stratigraphy, lithology and clay mineralogy to the Knollenmergel and Feuerletten Formations in Southern and Central Germany

PeerJ PrePrints | http://dx.doi.org/10.7287/peerj.preprints.325v1 | CC-BY 4.0 Open Access | received: 30 Mar 2014 | published: 30 Mar 2014

(Finckh, 1912; Matter et al., 1988), and Eastern France (Weishampel & Westphal, 1986). The Upper Variegated Marls at Frick mainly consist of reddish, grayish or greenish marls commonly containing carbonate concretions or layers (Sander & Klein, 2005). There are three horizons producing dinosaur remains (pers. comm. Dr. Benedikt Pabst, 2012), the lowermost of which represents the *Plateosaurus* bonebed and was the subject of the study by Sander (1992). The lowermost horizon is also the source of the material sampled histologically (Sander & Klein, 2005) and of the juvenile material described in this study.

The miring hypothesis of *Plateosaurus* bonebed origin

Mass accumulations of prosauropod remains in Frick, but also Halberstadt and Trossingen in Germany, share the same taphonomy, resulting in their description as *Plateosaurus* bonebeds (Sander, 1992). The sediments encasing the bones in all three localities are alluvial mudstones overprinted by pedogenesis, representing a floodplain in a semiarid climate. Apparently, *Plateosaurus* individuals as the heaviest animals in the environment were preferentially mired in shallow depressions when the mud was wet, acting as a deadly trap. Once the animal got stuck in the soft ground, trying to pull itself out, the mud liquified and the resulting undertow made it impossible to get out. This process happened several times over a long period, explaining the mass accumulations (Sander, 1992), which cannot be shown to represent mass death events, however. Sander (1992) noted the lack of animals of less than 5 m total body length and of juveniles in all *Plateosaurus* bonebeds. He suggested that this lack was due to smaller body size and the resultant negative scaling of the load on the juvenile feet, reducing the risk for animals of less than 5 m in body length to become mired. The miring hypothesis of Sander (1992) predicted that no juveniles would be found in *Plateosaurus* bonebeds. Until 2011 this prediction was not violated,

although the discovery by Sander & Klein (2005) of developmental plasticity opened up the possibility that juveniles exceeding 5 m in body length would be found.

Nevertheless, it came as a surprise that juvenile remains of *Plateosaurus* were found in the locality Frick in 2010 and particularly 2011. The 2011 material represents the remains of at least two individuals and primarily consist of isolated neural arches found in a bone field catalogued as MSF 11.3. in the lowermost bone layer. The term 'bone field' had been introduced by Sander (1992).

Ontogenetic studies of sauropodomorph dinosaurs: bone histology and suture closure

In general, there are only two methods to ascertain the postnatal ontogenetic stage in a dinosaur individual: bone histology and suture closure patterns, particularly in the skull and the vertebral column.

The long bone histology of *Plateosaurus engelhardti* from the localities of Trossingen and Frick has been studied in more detail (Sander & Klein, 2005; Klein & Sander, 2007) than any other basal sauropodomorph including *Massospondylus carinatus* (Chinsamy, 1993). The primary bone of *Plateosaurus engelhardti* consists of fibrolamellar bone tissue, indicating fast growth, but also reveals growth cycles demarcated by LAGs (lines of arrested growth). More importantly, the histological ontogenetic stage of similar sized individuals shows great variation (Sander & Klein, 2005), indicating a poor correlation between body size and age, suggesting developmental plasticity (Sander & Klein, 2005) with growth probably being influenced by environmental factors. The basal sauropodomorph *Massospondylus carinatus* does not seem to show such plasticity (Chinsamy, 1993; Chinsamy-Turan, 2005).

On the other hand, the histology of sauropod long bones received a great deal of attention (Curry, 1999; Sander 1999; Sander, 2000; Sander & Tückmantel, 2003; Curry & Erickson,

PeerJ PrePrints | http://dx.doi.org/10.7287/peerj.preprints.325v1 | CC-BY 4.0 Open Access | received: 30 Mar 2014, published: 30 Mar 2014

2005; Sander, Mateus & Knötschke, 2006; Klein & Sander, 2008; Sander et al., 2011). Sauropods revealed a fast-growing bone tissue, described as laminar fibrolamellar bone and a generally uniform histology. They grew along a genetically determined growth trajectory with a certain final size. Sauropods display a good correlation between body size/ontogentic stage and age with little individual variation in rate of growth and final size (Sander, 2000; de Ricqlès, Padian & Horner, 2003; Sander & Klein, 2005; Sander et al., 2011).

Yet another vertebral feature is important to determine osteological maturity: the stage of closure in the neurocentral suture between the neural arch and its centrum. Brochu (1996) observed different maturity stages in extant and extinct crocodilians by studying the neurocentral suture closure as an size-independant maturity criterion. He pointed out the presence of three different stages of neurocentral suture closure: open, partially closed and completely closed. The pattern of neurocentral suture closure plays another important role. In different groups and also within onmire group different patterns of closure can be found.

Within Sauropodomorpha basal sauropodomorphs like *Thecodontosaurus caducus* (Yates, 2003) and *Unaysaurus tolentinoi* (Leal et al., 2004) seem to show a pattern consistent with a posterior-anterior pattern of suture closure. Unfortunately the study on a close relative to *Plateosaurus*, *Massospondylus carinatus*, does not give a reliable pattern of a neurocentral suture closure due to the incompleteness of the material of also different specimens (Cooper, 1981). Recently described material of a juvenile prosauropod *Yunnanosaurus robustus* (Sekiya et al., 2013) indicates a roughly posterior-anterior pattern of suture closure. Within Sauropoda diverse patterns of suture closure can be recognized with different centers of ossification and in some cases with no visible order (Ikejiri, 2003; Ikejiri, Tidwell & Trexler, 2005; Gallina, 2011)

Objectives of study

The current study has three objectives: to describe and compare juvenile neural arch morphology of *Plateosaurus*, to test the hypothesis of developmental plasticity, and to test the miring hypothesis of *Plateosaurus* bonebed origins. We first give a detailed morphological description of neural arch morphology (laminae and fossae) of the immature isolated neural arches found in bone field MSF 11.3. and compare it with the neural arch morphology of osteological mature specimens of *Plateosaurus*. To address developmental plasticity, we need to determine individual body size. Since no femora from bone field 11.3. can be reliably associated with the isolated neural arches, morphometric analysis of the neural arches was used to calculate femur lengths of the juveniles as a proxy of body size. Femur lengths of the juveniles was then added to the Frick dataset on which the hypothesis of developmental plasticity was based. We thus tested if developmental plasticity is also reflected by the morphology of *Plateosaurus engelhardti* and not only in its histology. Finally, we evaluate the implications of the finds of juveniles for the miring hypothesis.

Institutional abbrevations

MSF, Sauriermuseum Frick, Frick, Kanton Aargau, Switzerland; **NAA**, Naturama, Aarau, Kanton Aargau, Switzerland; **SMA**, Sauriermuseum Aathal, Aathal, Kanton Zurich, Switzerland; **SMNS**, Staatliches Museum für Naturkunde, Stuttgart, Germany.

Material

The juvenile specimens of *Plateosaurus* were excavated in the Gruhalde clay pit of the Tonwerke Keller AG in Frick (Switzerland) as part of a bone field in 2011. The discovery was part of systematic paleontological excavations preceeding clay mining each year since 2004. Already in 2010, a seemingly juvenile individual had been discovered but this specimen

PeerJ PrePrints | http://dx.doi.org/10.7287/peerj.preprints.325v1 | CC-BY 4.0 Open Access | received: 30 Mar 2014, published: 30 Mar 2014

remains unprepared. Since the bone field yielding the 2011 juveniles was the third bone concentration encountered in the 2011 field season, the bones received consecutive collection numbers starting with "MSF 11.3.". The site was destroyed by mining but the exact position of the bonefield was recorded (Swiss State Coordinates: 642 953.5 / 261 961, lowermost bone layer, 80 – 90 cm above base of the gray beds). Bone field 11.3. yielded several different juvenile bones besides the studied juvenile neural arches, namely isolated centra. These were not used for further analyses because they lack diagnostic features, making a reliable determination of the position within the vertebral column impossible. Vertebrae belonging to the caudal vertebral series were not included to this study because the neurocentral sutures were closed in all specimens. In addition, tail vertebrae can only be assigned to a general region in the tail and not to an exact position. Caudal vertebrae, however, will be considered in terms of morphological change during ontogeny later on.

The girdle skeleton of the juvenile individuals is represented by a right scapula, right coracoid, a right pubis, a left ischium, and the appendicular skeleton is represented by a left femur, a tibia, a fibula, a left humerus, and a radius. These bones probably derive from immature individuals since the sheer size/length of the bones is much smaller than in adults. The articular surfaces at proximal and distal ends of appendicular bones still show an immature stage of ossification. A host of ribs and haemapophyses may also derive from the juveniles. This study focuses on the isolated neural arches from bone field 11.3. The sample includes 17 specimens of isolated neural arches belonging to the cervical and dorsal vertebral series (Table 1).

During the excavation, bone field 11.3. was covered with transparent foil to document the position of the bones found. This map shows that all bones were distributed over the whole area with no recognizably articulation or connection to each other (Fig. S1). The next step was to ascertain how much animals are represented and if specimens of different ontogenetic stage are recognizable. There are at least one adult and two juvenile animal represented by

206 bonefield 11.3.

207

208 **Preservation of the neural arches**

209 The preservation of the bones in bone field 11.3. is characterized by various degrees and
210 directions of diagenetic compactions, making the description of the neural arches sometime
211 challenging. The preservation ranges from no obvious compaction to slight dorsolateral
212 pressure and heavily dorsolateral pressure with three dimensional preservation (see
213 description of neural arches). The most obvious feature are fractures, going through the
214 bones. Some of the neural arches and other bones like the ischium show another new feature,
215 which has not been seen before in material from Frick: dessication cracks originating from the
216 bone lying on the surface for some time, which are filled in with a ferrous mineral during
217 diagenetic processes (see Fig. S2 D-E, Fig. S4 A, Fig. S5A, Fig. S9 A-C, Fig. S10 B-C, Fig.
218 S11 A-C, Fig. S13 B-C, Fig. 4).

219

220 **Adult specimens studied for comparison**

221 A morphological comparison of the studied juvenile specimens to other specimens,
222 especially osteological mature individuals, is important. This may reveal ontogenetic
223 morphological variation (Carballido & Sander, 2013). We studied three *Plateosaurus*
224 vertebral columns in detail for comparison. Two of these are from Frick (MSF 5, MSF 23)
225 and one is from Trossingen (cast of SMNS 13200), see Fraas (1913), Huene (1926), Galton
226 (1985a), Galton (1986), and Sander (1992) on this material.

227 Specimen MSF 5 consists of a block with two incomplete individuals of *Plateosaurus*,
228 with the smaller animal lying on the top of a larger one. The larger animal (MSF 5B)
229 preserves the anterior half of the skeleton with a partial and partially disarticulated skull,
230 articulated cervicals, the fifth dorsal vertebra and several ribs

disarticulated elements as shown in Fig. 1 (Rieber, 1985; Galton, 1986; Sander, 1992). The smaller individual (MSF 5A) is represented by a left humerus being smaller compared to the right humerus of the big animal lying on the right side of the block. The remains are preparated right-side up and still remain in the sediment (Sander 1992). The specimen is exhibited in situ at the Sauriermuseum Aathal (SMA) on permanent loan from the MSF. For this study the complete cervical and partly preserved dorsal vertebrae series of MSF 5B is of interest. MSF 5B represents the most complete and best preserved articulated cervical and partial dorsal series from the second cervical vertebra (C2) to the fifth dorsal vertebra (D5) found in Frick, anterior body regions being underrepresented due to the specific taphonomy of the locality (Sander 1992). The bones did not suffer much distortion compared to the bone field 11.3. specimens and are well preserved in three dimensions. All of the vertebrae of MSF 5B show completely closed neurocentral sutures. The neural arches show well and fully developed laminae and fossae throughout the vertebral series with no feature missing.

MSF 23 is a nearly complete and essentially articulated skeleton of a *Plateosaurus* from Frick, on display at the Sauriermuseum Frick (Sander, 1992) (Fig. 2). The morphology of the skeleton has not yet been described in detail, but it was figured by Sander (1992, fig. 3) as well as in the non-technical literature (Sander, 1993; Sander, 2012). The vertebral column is not complete. The segment of C1 to C6 is articulated but separated by a fault from C8 to D15 that follow in full articulations. Apparently the seventh cervical vertebra is missing. The absence of C7 may be due to the fault or because MSF 23 had been excavated in three blocks with C7 getting destroyed. Another reason for the missing vertebra might be that MSF 23 just had one vertebra less than other plateosaurs, possibly as a species-level difference. At a first glance, D15 may be considered to belong to the sacrum, being a dorsosacral, because it seems to be fused with the ilia on both sides. However no other *Plateosaurus* revealed more than three sacrals (Jaekel, 1914a; Galton, 1999; Galton, 2001). The diapophyses of D15 also are not as massive in their morphology as those of the sacrals. So the adhesion of D15 to the

PeerJ PrePrints | http://dx.doi.org/10.7287/peerj.preprints.325v1 | CC-BY 4.0 Open Access | received: 30 Mar 2014, published: 30 Mar 2014

anteriormost part of the sacrum may be due to the age of the animal. The neural arches in MSF 23 generally experienced strong dorsolateral pressure from the right side during diagenesis. This led to extreme deformation of the vertebrae in the specimen. Nevertheless MSF 23 shows fully developed vertebral morphology with all laminae and fossae being present. All of the neurocentral sutures are completely closed.

The third specimen is a cast of a complete skeleton from Trossingen (SMNS 13200, Fig. 3), exhibited at the Naturama (NAA) in Aarau (Switzerland). SMNS 13200 was excavated as nearly complete articulated skeleton in 1911 in the Knollenmergel Beds of Trossingen at the Obere Mühle (Fraas, 1913) and forms the basis of the osteological description by Huene (1926). The left forelimb distal to the humerus is missing, and the tail is incomplete as well, missing some vertebrae. However, the presacral vertebral column is complete and well preserved. SMNS 13200 shows good three dimensional preservation with no or little influence of compaction on the whole complete vertebral column. All vertebrae display well developed laminae and fossae with all neurocentral sutures being closed.

Methods

The morphological description of the neural arches follows the nomenclature of Wilson (1999) and Wilson et. al (2011). Because of their complex morphology and because morphological characters change sequentially throughout the axial skeleton (Carballido et al., 2012; Carballido & Sander, 2013), sauropodomorph neural arches can be assigned to specific positions in the vertebral column with a margin of error of one position or less. In sauropods, not only do vertebral characters change within one animal but also during the ontogeny of the same animal (Carballido et al., 2012). Before a sauropod reached osteological maturity, its vertebrae passes developmental stages, often displaying more primitive characters known in more basal taxa. To determine the stage of osteological maturity of the juvenile *Plateosaurus*

PeerJ PrePrints | http://dx.doi.org/10.7287/peerj.preprints.326v1 | CC BY 4.0 Open Access | received 30 Mar 2014, published 30 Mar 2014

a direct comparison of morphological characters to osteological mature (completely closed neurocentral sutures) plateosaurs is necessary.

Terminology of laminae and fossae

The morphological description of the neural arches of this study follows the nomenclature of Wilson (1999) for the laminae and Wilson et al. (2011) for the fossae of sauropod dinosaurs which can be applied to basal sauropodomorphs as well (Wilson, 1999; Wilson et al., 2011). The nomenclature for laminae set by Wilson (1999) is based on landmarks on the vertebra, namely the connections a lamina establishes, whereas the nomenclatures set before by other scientists were mainly based on the origin the laminae have. The fossae's names are defined by the surrounding laminae (Wilson et al., 2011).

Morphometrics

Simple morphometric analysis was applied to estimate the body length of the juvenile *Plateosaurus* from measurement that can be taken on neural arches. In dinosaurs, femur length is a reliable proxy for body mass (Carrano, 2006). In the case of *Plateosaurus* the femur lengths equals approximately 1/10 of body length (Sander, 1992). Since our material only consists of isolated neural arches, we needed to establish a new proxy which is suitable for determining the body lengths of the juveniles. We decided to use the zygapophyseal lengths of the neural arches for developing a proxy. Due to the extreme dorsolateral compression of some specimens and the better preservation of the pre- and postzygapophyses compared to the transverse processes of the neural arches, measuring zygapophyseal length appears to be the most reliable size proxy. The zygapophyseal length of the neural arches of all specimens studied was measured from the tip of the prezygapophysis to the tip of the postzygapophysis, representing the maximum anteroposterior length of a neural arch. For

PeerJ PrePrints | http://dx.doi.org/10.7287/peerj.preprints.325v1 | CC-BY 4.0 Open Access | received: 30 Mar 2014, published: 30 Mar 2014

the calculations of body lengths of the juveniles, femur length of specimens MSF 5B, MSF 23 and SMNS 13200 was measured (Table 2) as maximal length on the medial side. The femur of specimen MSF 5B is not preserved, but its scapula is. Based on the scapula/femur ratio (76%) of specimen MSF 23 and on measured scapula length of MSF 5B, we were able to calculate the femur length of MSF 5B.

The ratio between zygapophyseal length and femur length of MSF 5B, MSF 23, and SMNS 13200 were measured to calculate the femur lengths of the juvenile specimens of bone field 11.3. (Table S2). For the calculation of the femur lengths of the juveniles in percentage, we only used data of specimen SMNS 13200, where the material is the most complete and best preserved one, compared to all other specimens studied.

The main problems during measurements of zygapophyseal lengths in neural arches of all specimens studied were caused by poor preservation in some bones, with the tips of pre- or postzygapophyses missing. Sometimes heavy deformation, e.g., in MSF 23 in the region of the posteriormost dorsal vertebrae, made measurements impossible. In partly articulated specimens like MSF 5B and MSF 23, bones like dorsal ribs and gastralia obscure parts of the vertebral column.

Morphometric measurements were performed with a sliding caliper for distances between 0-150 mm. If the distance was greater than 150 mm, or the measurement was not accessible with the sliding caliper, a measuring tape was used. The measurements were taken to the nearest 0.1 mm (calliper) and to the nearest millimeter (measuring tape).

Anatomical abbrevations

acdl, anterior centrodiapophyseal lamina; **acpl**, anterior centroparapophyseal lamina; Cd?, caudal of indeterminate position; **cdf**, centrodiapophyseal fossa; **cpol**,

PeerJ PrePrints | http://dx.doi.org/10.7287/peerj.preprints.325v1 | CC-BY 4.0 Open Access | received: 30 Mar 2014, published: 30 Mar 2014

centropostzygapophyseal lamina; **cprl**, centroprezygapophyseal lamina; **C1**, atlas; **C2**, axis; **C3**, third cervical; **C4**, fourth cervical; **C6**, sixth cervical; **C7**, seventh cervical; **C8**, eighth cevival; **C10**, tenth cervical; **C?**, cervical of indeterminate position; **d**, diapophysis; **D3**, third dorsal; **D4**, fourth dorsal; **D5**, fifth dorsal; **D6**, sixth dorsal; **D7**, seventh dorsal; **D10**, tenth dorsal; **D11**, eleventh dorsal; **D15**, fifteenth dorsal; **D?**, dorsal of indeterminate position; **pa**, parapophysis; **pcdl**, posterior centrodiapophyseal lamina; **poz**, postzygapophysis; **pocdf**, postzygapophyseal centrodiapophyseal fossa; **podl**, postzygodiapophyseal lamina; **ppdl**, paradiapophyseal lamina; **prz**, prezygapophysis; **prcdf**, prezygapophyseal centrodiapophyseal fossa; **prdl**, prezygodiapophyseal lamina; **spol**, spinopostzygapophyseal lamina; **sprl**, spinoprezygapophyseal lamina; **tprl**, intraprezygapophyseal lamina; **tpol**, intrapostzygapophyseal lamina; **zyga**, zygantrum; **zygo**, zygosphene.

Results

Description

Among the juvenile bones, there are six isolated neural arches (specimens MSF 11.3.074, MSF 11.3.258, MSF 11.3.317, MSF 11.3.366, MSF 11.3.371, and MSF 11.3.388, see also Table 1 and Supplemental Information) that can be assigned to the cervical vertebral column. This is based on their low and elongated appearance in comparison to the taller and shorter proportions of the dorsal neural arches (Huene, 1926). We identified eleven dorsal neural arches from the bone field 11.3. sample (specimens MSF 11.3.049, MSF 11.3.067, MSF 11.3.095, MSF 11.3.107, MSF 11.3.167, MSF 11.3.169, MSF 11.3.241, MSF 11.3.303, MSF 11.3.339, MSF 11.3.360 and MSF 11.3.376, see Table 1 and Supplemental Information). The specimens can be further subdivided into anterior (C1 to C5) and posterior (C6 to C10) cervical neural arches and into anterior (D1 to D5), middle (D6 to D10) and posterior (D11 to

PeerJ PrePrints | http://dx.doi.org/10.7287/peerj.preprints.325v1 | CC-BY 4.0 Open Access | received: 30 Mar 2014, published: 30 Mar 2014

D15) dorsal neural arches. The identification of the position of the neural arches are performed with the help of characters and features of diapophyses (d), prezygapophyses (prz), postzygapophyses (poz), parapophyses (pa), and the neural spines, as described by von Huene (1926) and Bonaparte (1999). The laminae and fossae play an important role in the morphology of the neural arch (Bonaparte, 1999; Wilson, 1999; Wilson et al., 2011). Furthermore the processes of the neural arch change gradually along the vertebral column, e.g. in length, shape, size, location on the arch and angle at which these stand out from the vertebra (Wilson, 1999).

The complete vertebral column of *Plateosaurus engelhardti* consists of a rudimentary proatlas, 10 cervical vertebrae, 15 dorsal vertebrae, three sacral vertebrae, and at least 50 caudal vertebrae (von Huene, 1926; Bonaparte, 1999; Upchurch, Barrett & Galton, 2007). Specimens MSF 11.3.388 (cervical neural arch) and MSF 11.3.169 (dorsal neural arch) displayed the worst preservation and were not described in detail. We were unable to reliably determine the position of these two arches within the vertebral column since all of the important characters were net preserved.

Cervical neural arches

Axis, **MSF** 11.3.317 (Fig. S2 A-C)

The axis is the anteriormost neural arch identified in the bone field. With the diapophysis and parapophysis missing, the diapophyseal and parapophyseal laminae are not present in the axis. The prezygapophysis shows much smaller and shorter facets than the postzygapophysis. The prezygapophysis is ventrally supported by a single cprl. The tprl connecting both prezygapophyses is missing. Short sprl's line up dorsally to the neural spine. As a counterpart

PeerJ PrePrints | http://dx.doi.org/10.7287/peerj.preprints.325v1 | CC-BY 4.0 Open Access | received: 30 Mar 2014, published: 30 Mar 2014

379 the cpol holds up the postzygaphysis, and the spol runs up dorsally from the postzygapophysis
380 towards the neural spine. A poorly developed tpol connecting the postzygapophysis is
381 present. The only fossa is the spof, but it does not extend deeply into the neural arch. In
382 ventral view, the pedicels show the zipper-like surface of the neurocentral suture, which is
383 typical for morphologically immature bones originating from the open neurocentral suture
384 (Brochu, 1996; Irmis, 2007). Further on, the articular surfaces of the poz's in ventral view are
385 abrasive and were only partly ossified at the time of death. The morphology of the axis arch
386 does not differ from the adult condition as described by von Huene (1926).

387

388 Third cervical, **MSF** 11.3.258 (Fig. S2 D-F)

389 The neural arch can be assigned to the third position within the vertebral column. No
390 diapophysis or parapophysis is present, therefore the arch is missing any diapophyseal and
391 parapophyseal laminae. Postzygapophysis and prezygapophysis are both small and form a
392 low angle, indicating that this neural arch is an anterior cervical one. The tprl (the connecting
393 lamina between the prezygapophyses) and tpol is well developed. The sprl is hardly
394 developed in contrast to the spol being quite present. The cprl and cpol are well developed.
395 Like in the axis, the spof is present and becomes deeper. Though less developed, the sprf is
396 present now. Zipper-like suture surfaces on the pedicels are recognizable in ventral view.

397

398 Fourth cervical, **MSF** 11.3.371 (Fig. S3 A-E)

399 The arch shows a partly preserved diapophysis on the right lateral side, but still no
400 parapophysis is present. Nevertheless, diapophyseal as well as parapophyseal laminae do not
401 extend onto the arch. The prezygapophyses of MSF 11.3.371 are much more elongated
402 compared to prezygapophyses in more anterior neural arches and the postzygapophyses of the

PeerJ PrePrints | http://dx.doi.org/10.7287/peerj.preprints.335v1.1 CC-BY 4.0 Open Access | received: 30 Mar 2014 | published: 30 Mar 2014

same arch. The surfaces of the articular surfaces have a quite low angle of less than 45°. While the cpol remains short in length, the cprl is a thick elongated lamina. Sprl and spol are well developed along with the sprf and the spof, with the spof being the deeper and broader fossa. Other fossae are not present.

Sixth Cervical, **MSF** 11.3.074 (Fig. S4 A-B)

The partly preserved diapophysis fully moved dorsally onto the neural arch and is situated at the midlength of the neural arch. No parapophysis is present. The prezygapophysis and postzygapophysis seem to be very steeply angled, and the surface of the articular facets is rough, suggesting a cover by cartilage. This is unlike in adults, where zygapophyseal articular facets are well ossified and smooth. Intense lateral compaction of the arch with a sligthly ventral to dorsal shift is recognizable. The acdl emerges as a thin lamina going anterodorsally up from the anterior part of the junction between centrum and neural arch to the tip of the prezygapophysis, recognizable on both the left and right lateral side; concomitant with the presence of a small and shallow prcdf. The pcdl is not present. The neural spine is higher than in the anterior cervicals. Sprl, spol, tprl and tpol are present. Both cprl and cpol seem to be shorter than in the more anterior cervical arches. The sprf is not well developed whereas the spof is deeper. The pedicels lack the zipper-like structures due to poor preservation.

Tenth cervical, **MSF** 11.3.366 (Fig. S5 A-B)

In the tenth cervical neural arch the cervicodorsal transition is visible. Posteriormost cervical neural arches show strong reduction in centrum and zygapophyseal length in comparison to the previous arches. The neural spine gets higher. The size, shape and functions of diapophyses change due to dorsal ribs which have to be supported. The ribs are

PeerJ PrePrints | http://dx.doi.org/10.7287/peerj.preprints.325v1 | CC-BY 4.0 Open Access | received: 30 Mar 2014, published: 30 Mar 2014

supported from below by parapophyses which migrate onto the dorsal neural arches (Wilson, 1999). Though the diapophysis of the specimen is not complete with the tip missing, the diapophysis arises fully from the neural arch. As a consequence, all of the diapophyseal laminae are present and well developed. These include the acdl, which is a thin lamina in the sixth cervical (MSF 11.3.074), but which is thickened and well established in specimen MSF 11.3.366. The diapophysis is well supported ventrally by the pcdl, being the stronger and broader lamina, and the acdl. The cdf is still simple and not deep. On the contrary, the prcdf and pocdf are deep and extensive. The surface of the prezygapophyses and postzygapophyses are much more extensive, which is not the case for zygapophyses of anterior cervicals. Still, a parapophysis is not visible, but the laminae connecting the diapophysis with the prezygapophysis (prdl) and the diapophysis with the postzygapophysis (podl) are distinctly developed. All the other laminae like sprl, spol, tprl, tpol, cprl and cpol as well as sprf and spof are well developed. In contrast to the neural spine of more anterior cervicals, the neural spine of this specimen is much thicker. Specimen MSF 11.3.366 is the anteriormost specimen in the cervical series to exhibit a zyposphene and zygantrum for further support of the vertebral column.

Dorsal neural arches

Anterior neural arches from the first to the seventh dorsal are most abundant in bone field 11.3., and only two posterior dorsal neural arches can be recognized. Some positions are represented twice like the third, the fifth, the sixth and the tenth/eleventh dorsal. All of the dorsal neural arches show well developed zygosphenes and zygantra if this region is preserved. Zipper-like sutural surfaces are preserved for the dorsals MSF 11.3.360, MSF 11.3.167, MSF 11.3.095, MSF 11.3.107 and MSF 11.3.339.

PeerJ PrePrints | http://dx.doi.org/10.7287/peerj.preprints.325v1 | CC-BY 4.0 Open Access | received: 30 Mar 2014, published: 30 Mar 2014

Third dorsal, **MSF** 11.3.360 (Fig. S6 A-D)

This specimen is one of the most anterior dorsal neural arch in the dorsal series. With the shortest and thickest neural spine within the whole vertebral series, being nearly square in shape in dorsal view and sticking out from the arch at a right angle, the identification of this neural arch as a third dorsal is unmistakeable (Huene, 1926). The diapophysis is slightly oblique and gently posteriorly directed. Furthermore, three very deep fossae are well recognizable below the diapophysis (prcdf, pocdf and cdf). A first sign of a slight parapophysis articular facet is recognizable on both sides of the bone. The parapophysis still seems to have been located more on the centrum than on the neural arch. The much broader facets of the prezygapophyses in comparison to small ones of the postzygapophyses are remarkable. Nonetheless, both show rough articular sufaces like all the cervical neural arches. All laminae (acdl, pcdl, prdl, podl, sprl, spol, cprl and cpol) are fully developed.

Third dorsal, **MSF** 11.3.376 (Fig. S7 A-C)

Specimen MSF 11.3.376 can also be identified as a D3 due to the same diagnostic characters. However, there are some striking differences in comparison to the previous specimen. The prezygapophyses are much smaller and seem to be elongated instead of being broad. This may be due to preservation, though the shape of MSF 11.3.360 appears to be little affected by diagenetic deformation. MSF 11.3.376 experienced dorsoventral crushing. In addition, the parapophysis articular area has clearly developed and is situated on the neural arch while the parapophyses of MSF 11.3.360 still articulates with the centrum, because it is hardly visible. Commonly, the parapophyses first come in contact with the acdl in the fifth or sixth dorsal (von Huene, 1926). All laminae are fully present and developed, whereas the acdl is slightly truncted by the parapophysis articular facet.

PeerJ PrePrints | http://dx.doi.org/10.7287/peerj.preprints.325v1 | CC-BY 4.0 Open Access | received: 30 Mar 2014, published: 30 Mar 2014

Fourth dorsal, **MSF** 11.3.049 (Fig. S8 A-B)

In the fourth dorsal neural arch, the thickness of the spine decreases a little and the spine gets longer. Unfortunately the tip of the diapophysis is missing on both sides. No parapophysis is visible. In all likelihood, the parapophysis articular facet is situated on the centrum. This may lead to the assumption that we deal with a cervical, but the neural spine indicates the specimen to be a dorsal. The appearance of the prezygapophyses and the very short postzygapophyses also argue for a dorsal neural arch. Fossae and accompanying laminae are well developed. All three fossae below the diapophysis are very deep and well visible (prcdf, cdf and pocdf). No parapophysis influences the laminae and fossae existent. Tough the cdf seems to be not as deep as in the third dorsals, though. The well established laminae and fossae indicate the neural arch to belong to a forth dorsal. Cprl and cpol distinctly arise from the prezygapophysis and postzygapophysis, increasing the general height of the neural arch.

Fifth dorsal, **MSF** 11.3.067 (Fig. S9 A-C)

The fifth dorsal neural arch shows partly preserved diapophyses, but no parapophysis articular facet due to poor preservation. The neural spine shows that a posterior inclination is seen from now on backwards in the vertebral column. The left lateral side of the arch shows that all the laminae and fossae are well developed in this specimen. As expected, the prcdf begins to diminish in size and extent due to the parapophysis articular facet moving dorsally onto the neural arch, also slowly closing the acdl, separating the lamina into acpl and ppdl in posterior dorsal neural arches. In addition, the parapophysis articular facet also influences the prdl to the extent that it forms back. This process takes place stepwise, visibly beginning in

499 the fifth dorsal and being complete in the eigth dorsal in which there are only two fossae left
500 below the diapophysis (pocdf and cdf).

501

502 Fifth dorsal, **MSF** 11.3.167 (Fig. S10 A-C)

503 This is another neural arch belonging to a fifth dorsal vertebra. The specimen is heavily
504 crushed on the left side, leaving the right side for the description. All laminae are well
505 developed beneath the diapophysis with deep fossae (pcdl, acdl, prdl, podl, sprl, spol, cprl and
506 cpol). A parapophysis articular facet is present interrupting the acdl. The appearance of the
507 zygapophyses conforms with those of specimen 11.3.067.

508

509 Sixth dorsal, **MSF** 11.3.095 (Fig. S11 A-C)

510 Specimen MSF 11.3.095 is assigned to the sixth position in the dorsal vertebral column.
511 The diapophyses are posteriorly oriented, suggesting a middle dorsal neural arch. The
512 prezygapophyses are elongated in contrast to the postzygapophyses being shorter and smaller
513 in expanse. Furthermore all laminae are fully developed. At the anterior end of the arch,
514 dorsal of the neurocentral suture, a distinctive parapophysis articular facet is present on both
515 sides. The parapophysis articular facet displaces the acdl, giving rise to the ppdl, connecting
516 the parapophysis from ventral to dorsal with the diapophysis, and the acpl and the prpl. The
517 prpl connects the parapophysis anterodorsally with the prezygapophysis. The prdl is still well
518 visible. All the rest of the laminae are well developed, like in the arches described before. The
519 same applies to all of the fossae. Further evidence for the identification of the specimen as a
520 sixth dorsal is that the prcdf becomes narrower and decreases in depth compared to the prcdf
521 in more anterior neural arches.

Sixth dorsal, **MSF** 11.3.107 (Fig. S12 A-C)

This specimen can also be identified as a sixth dorsal neural arch. All features seen in this specimen coincide with those of specimen MSF 11.3.095. The bone is complete although the diapophysis is broken off on the left side and is diagenetically recemented to the arch.

Seventh dorsal, **MSF** 11.3.339 (Fig. S13 A-C)

Although being the most complete and best preserved specimen of all, this neural arch is strongly influenced by anteroposterior compaction. This implies an extremely posteriorly directed diapophysis and a constrained elongation of the prdl on the right lateral side. Aside from the preservation, the prdl is much shorter and more inconspicuous than in the more anterior neural arches which argues for a position around the seventh dorsal, where the prdl is fused with the ppdl, the acdl is consumed by the acpl, and the cprl is disrupted by the prpl, connecting the parapophysis anterodorsally with the prezygapophysis. Unfortunately, no parapophysis articular facet is preserved. Furthermore, the specimen impressively shows the rough and only partly ossified zygapophyseal articular surfaces.

Tenth/Eleventh dorsal, **MSF** 11.3.241 (Fig. S14 A-C)

This is the posteriormost position represented by the neural arches found in bone field 11.3., being the tenth or eleventh dorsal neural arch. The arch has broad and extensive diapophyses, oriented nearly at right angless to the arch. The partly preserved neura spine does not show any indication of a bifurcation in the posterior part, which is mainly the reason why the arch cannot be assigned to the 12th up to the 15th dorsal. A sure indicator for a posterior dorsal position are the presence of only two fossae below the diapophyses. The prdl

has fully vanished from the arch in this position. A parapophysis articular facet is well preserved on the left lateral side of the specimen. Prezygapophyses and postzygapophyses are both short compared to prezygapophyses and postzygapophyses in the middle dorsal neural arches (i.e., the fifth, sixth, and seventh dorsal). In all middle and posterior dorsal neural arches, the articular surfaces of the zygapophyses are horizontal. At the same time, the zygosphene and zygantrum are very distinctive.

Tenth/Eleventh dorsal, **MSF** 11.3.303 (Fig. S15 A-C)

This posterior dorsal neural arch can also be assigned to a position around the tenth dorsal. The diapophyses are not well preserved, missing the tip on the right lateral side and not being preserved on the left lateral side, to which a partly preserved bone (MSF 11.3.304) is cemented. Presumably this bone is a posterior caudal vertebra. Again the diapophysis is directed laterally at a 90-degree angle like in specimen MSF 11.3.241. The shape and appearance of the prezygapophyses and postzygapophyses also coincide with those of the previously described specimen. In contrast to specimen MSF 11.3.241, the postzygapophyses show completely ossified articular surfaces. All laminae and fossae are well developed (acpl, ppdl, pcdl, podl, sprl, spol, tprl, tpol, cprl and cpol).

Minimal number of individuals (MNI)

The assignment to position of the neural arches indicates the minimum number of juvenile individuals (MNI) represented in bone field MSF 11.3. In the dorsal series, some positions are represented twice, such as the the third dorsal (MSF 11.3.360 and MSF 11.3.376), the fifth dorsal (MSF 11.3.067 and MSF 11.3.167), the sixth dorsal (MSF 11.3.095

and MSF 11.3.107), and the tenth/eleventh dorsal (MSF 11.3.241 and MSF 11.3.303). The MNI of juvenile *Plateosaurus* from bone field 11.3. is thus two.

Morphometric analysis

Neural arch size measured as zygapophyseal length

The values of zygapophyseal length of the isolated neural arches pertaining to juveniles and described here and of the specimens MSF 5B, MSF 23 and SMNS 13200 were measured for morphometric analysis (Table S1). The trend of zygapophyseal lengths along the cervical and dorsal series shows a clear pattern in all adult specimens studied (MSF 5B, MSF 23 and SMNS13200) (Fig. 5). This pattern is roughly followed by the disarticulated neural arches from bone field 11.3 as well. The anterior cervical neural arches show a rapid increase in zygapophyseal length, with C4/C5 showing the maximal length. Posteriorly, a decrease in the length of the cervical neural arches takes place, with the anterior dorsals (D3) showing the lowest value of zygapophyseal length. Subsequently the zygapophyseal length again increases, though at a much lower rate than in the anterior cervicals. The comparison of neural arches at the same positions suggests that the two juvenile individuals are of a slightly different size. The maximal size difference is approximately 20%.

Specimen SMNS 13200 with the greatest femur length (685 mm) generally possesses the greatest zygapophyseal lengths. Except for a few outliers, its lengths are clearly greater in comparison to the other specimens. Though specimen MSF 23 is the second largest individual on the basis of a femur length of 610 mm, the zygapophyseal lengths of the slightly smaller MSF 5B (calculated femur length of 565 mm), overlap with those of MSF 23. Throughout the vertebral series, the zygapophyseal lengths of the isolated neural arches are less than those of the adult specimens. The zygapophyseal lengths of the juveniles only overlap with those of

PeerJ PrePrints | http://dx.doi.org/10.7287/peerj.preprints.325v1 | CC-BY 4.0 Open Access | received: 30 Mar 2014, published: 30 Mar 2014

593 specimen MSF 23 in the cervical series which may be due to the strong deformation in MSF
594 23.
595
596 **Zyg/Fe ratios**
597 Zygapophyseal length was calculated as a percentage of femur length (Table S2) to
598 estimate femur length from the isolated neural arches (Table 3). With the help of these ratios,
599 it is possible to estimate femur length of the juvenile specimens, which is documented in
600 Table 3. Though the Zyg/Fe ratios of MSF 5B, MSF 23 and SMNS 13200 show a wide range
601 between 12.5 – 28.3 % (Table S2), they all reflect a pattern, following the regular change in
602 zygapophyseal length throughout the vertebral column visible in all specimens. The pattern of
603 increase and decrease of zygapophyseal lengths explains the wide range in the Zyg/Fe ratios
604 in these individuals. The calculated femur lengths of the two 11.3. individuals range from
605 478.9 to 594.9 mm, depending on position of the neural arch and size of the individual. Again
606 the variation in zygapophyseal length, which can be seen in all specimens studied, accounts
607 for the relative large variation in estimated femur length. Based on the vertebral positions that
608 are represented twice, the femur length estimate for the larger juvenile is between 539 mm
609 and 595 mm and that for the smaller juvenile is between 479 mm and 593 mm.

610 **Discussion**

611 **Ontogenetic changes in vertebral morphology**
612 Morphological changes through ontogeny in sauropodomorphs are poorly known because
613 juveniles are rarely found and are mainly represented by late juveniles to subadult specimens
614 (Ikejiri, Tidwell & Trexler, 2005; Tidwell and Wilhite, 2005). Until now there are just three
615 basal sauropodomorphs and two sauropods with embryos or very young specimens known:
616 *Massospondylus carinatus* (Reisz et al., 2005; Reisz et al., 2012), *Mussaurus patagonicus*

PeerJ PrePrints | http://dx.doi.org/10.7287/peerj.preprints.325v1 | CC-BY 4.0 Open Access | received: 30 Mar 2014, published: 30 Mar 2014

(Bonaparte & Vince, 1979; Otero & Pol, 2013), the basal sauropodomorph *Yunnanosaurus robustus* (Sekiya et al., 2013), a baby titanosauriform closely related to *Brachiosaurus* (Carballido et al., 2012), and *Europasaurus* (Sander et al. 2006; Marpmann et al., 2011; Carballido & Sander, 2013). The most detailed study of ontogenetic changes in vertebral morphology has been done on *Europasaurus holgeri*, with different ontogenetic stages being recognized and defined (Carballido & Sander, 2013). Though in most cases isolated bones and incomplete specimens of vertebral column remains exacerbate studies on morphological changes through ontogeny (Carpenter & MacIntosh, 1994; Foster, 2005).

Based on neural arch morphology, Carballido and Sander (2013) recognized five morphological ontogenetic stages: early immature, middle immature, late immature and two stages of maturity. In the early and middle immature stage, laminae and/or fossae of a neural arch are not fully developed. In the late immature stage all morphological characters of adults are already present, but the neurocentral suture remains open. The ontogenetic stage of the juvenile MSF 11.3. specimens equals the late immature stage found in *Europasaurus holgeri*.

The comparison of the morphology of cervical and dorsal neural arches between the juvenile MSF 11.3. specimens and the mature *Plateosaurus* did not reveal any differences at all. Laminae as well as fossae are all well developed in all osteologically mature individuals as well as in the juvenile *Plateosaurus* of bone field 11.3. The only distinction which can be made are the fully open neurocentral sutures in the 11.3. juveniles and the fully closed and invisible neurocentral sutures in the mature individuals (MSF 5B, MSF 23 and SMNS 13200).

The series of ontogenetic changes in the neural arch morphology as detected for *Tazoudasaurus* (Allain & Aquesbi, 2008), the brachiosaurid SMA 0009 (Carballido et al., 2012), *Phuwiangosaurus* (Martin, 1994) and especially the camarasauromorph *Europasaurus holgeri* in Carballido and Sander (2013) cannot be observed in *Plateosaurus*. While this may be due to the late ontogenetic stage of the juvenile specimens from bone field MSF 11.3, it may also be

PeerJ PrePrints | http://dx.doi.org/10.7287/peerj.preprints.325v1 | CC-BY 4.0 Open Access | received: 13 Mar 2014, published: 30 Mar 2014

plesiomorphy of basals sauropodomorphs. Basals sauropodomorphs are more plesiomorphic in their neural arch morphology than more derived sauropods and may have been more plesiomorphic in having less ontogenetic change in vertebral morphology. The function of laminae in sauropodomorphs was in the structural support of the neck and trunk region (Osborn, 1899; McIntosh, 1989), but also evolved as a correlate of axial pneumaticity (Seeley, 1870; Wilson, 1999; Taylor & Wedel, 2013). Most probably laminae can be explained by both factors.

Size and ontogenetic stage in *Plateosaurus*

The fully open neurocentral sutures of the neural arches described in this study are a reliable indicator for immaturity (Brochu, 1996). However, the calculated femur length for both juvenile individuals ranges between 479 mm and 595 mm, indicating that these were not smaller than many mature individuals from the Frick *Plateosaurus* bonebed. Histological mature animals from Frick and Trossingen studied in Sander and Klein (2005) display a femur length between 480 mm and 990 mm. The femur lengths of osteological immature, as well as osteological mature, specimens and histological mature animals merge into one another (Fig. 6). Furthermore comparing the osteological mature specimen MSF 5B (femur length: 565 mm) with the juveniles one can assume that the immature animals would have become larger than MSF 5B. Both this study and Sander and Klein's study in 2005 show no correlation between age and size. Developmental plasticity is not only observable in histology of *Plateosaurus*, but also corroborated by its morphology.

However, as discussed in the introduction, alternative explanations to developmental plasticity such as the presence of several *Plateosaurus* species represented at the locality of Frick cannot be excluded, and a combination of several hypotheses is probable. Different species populations separated in time,

PeerJ PrePrints | http://dx.doi.org/10.7287/peerj.preprints.325v1 | CC-BY 3.0 Open Access | received: 30 Mar 2014, published: 30 Mar 2014

and/or sexual dimorphism) still remain possible and cannot be tested without further detailed study of the material from the *Plateosaurus* bonebeds and the taphonomy of the bonebeds.

Patterns of neurocentral suture closure

The isolated neural arches from bone field MSF 11.3. contribute little to our understanding of the pattern of neurocentral suture closure in *Plateosaurus*. Circumstantial evidence consists of the lack of isolated posterior dorsal and caudal arches compared to the large number of caudal vertebrae preserved in the bone field. This is suggestive of suture closure beginning in the tail and posterior dorsal region. Further we missed most of posterior cervical neural arches (C7 to C9) in our sample size. Those, as well as posterior dorsals (D12 to D15) may have had completely closed neurocentral sutures and thus are present on bone field 11.3. We just could not assign them to belong to juveniles because the only reliable character for immaturity in our specimens (open neurocentral sutures) are not present. This indicates a pattern of suture closure with more than one ossification center.

Implications for taphonomic hypothesis

As noted, the taphonomic hypothesis for origin of the *Plateosaurus* bonebeds of Central Europe proposed by Sander (1992) predicted a size threshold for animals below which animals did not become mired. According to Sander (1992), this would explain the lack of juveniles because of their small size. While the discovery of juveniles in the lowermost bone horizon seemingly contradicts the hypothesis of Sander (1992), this is not the case. The juvenile *Plateosaurus* individuals described in this study are as large or even larger than the smallest fully grown *Plateosaurus* present at Frick, upholding the view that a size threshold existed that kept animals smaller than a 5-m *Plateosaurus* from becoming mired in the mud traps. This conclusion was implicit in the work of Sander & Klein (2005) and Klein & Sander

PeerJ PrePrints | http://dx.doi.org/10.7287/peerj.preprints.325v1 | CC-BY 4.0 Open Access | received: 30 Mar 2014, published: 30 Mar 2014

692 (2007), but it was not expressed because histological immaturity could not be properly
693 correlated with skeletal immaturity because isolated neural arches were not known from Frick
694 at the time.

695 Conclusions

696 The study focuses on the first remains of juveniles of the basal sauropodomorph
697 *Plateosaurus engelhardti*. *P. engelhardti* can be found in over 40 localities in Central Europe
698 (Sander, 1992). The juveniles studied come from the locality of Frick, one of three localities
699 preserving abundant remains of *Plateosaurus* and sharing the same taphonomy. These
700 localities were described as *Plateosaurus* bonebeds by Sander (1992). The juveniles were
701 found in a bone field in the lowermost bone horizon in the Gruhalde clay pit of the Tonwerke
702 Keller AG, revealing a concentration of several juvenile and adult bones. The most interesting
703 specimens were isolated neural arches, representing an MNI of two juveniles that slightly
704 differed in size. The juvenility and osteological immaturity of the remains can reliably be
705 linked to the lack of fusion of the neural arches to the centra (Brochu, 1996). The ventral
706 surface of the pedicel reveals the characteristic zipper-like surface of the suture, but the
707 morphology of the immature neural arches does not differ from the morphology of the
708 osteologically mature specimens (MSF 5B, MSF 23 and SMNS 13200) studied for
709 comparison. Thus, the juvenile specimens of *P. engelhardti* seem to represent late immature
710 individuals. Patterns of abundance in the bone field hint at suture closure pattern in
711 *Plateosaurus* from posterior to anterior. Though a pattern of suture closure with more than
712 one ossification center is possible.

713 Morphometric analysis based on the ratio of zygapophyseal length to femur length
714 indicates the femur length of the juvenile specimens to have been between 479 and 595 mm.
715 Thus these animals were larger than the smallest histologically fully grown individual with a

PeerJ PrePrints | http://dx.doi.org/10.7287/peerj.preprints.325v1 | CC-BY 4.0 Open Access | received: 30 Mar 2014, published: 30 Mar 2014

femur length of 480 mm from Frick (Sander & Klein 2005) and most probably would have become larger than another individual with a femur length of 565 mm. The morphometric analysis thus independently confirms the poor correlation between age and size in the finds from Frick assigned to *P. engelhardti*, most likely reflecting pronounced developmental plasticity of *Plateosaurus* (Sander & Klein 2005). However, alternative explanations such as the presence of several *Plateosaurus* species represented at the locality Frick cannot be excluded, and a combination of several hypotheses (developmental plasticity, different species, populations separated in time, and/or sexual dimorphism) still remain possible and cannot be tested without further detailed study of the material from the *Plateosaurus* bonebeds and the taphonomy of the bonebeds. Our study also failed to falsify the taphonomic miring hypothesis of Sander (1992) explaining the origin of the *Plateosaurus* bonebeds. While juvenile, the newly described individuals are not smaller than some adults and above the size threshold for miring.

Acknowledgments

We want to thank Dr. Benedikt Pabst (Sauriermuseum Aathal and Sauriermuseum Frick, Switzerland) for the loan and entrustment of the juvenile specimens, giving us the opportunity to do research on the first juveniles of *P. engelhardti* to be found. Our gratitude also goes to Dr. Rainer Foelix (Naturama in Aarau, Switzerland) and Monica Rümbeli (Sauriermuseum Frick, Switzerland) for enabling access to the specimens SMNS 13200 and MSF 23 for further study. We thank Olaf Dülfer and Martin Schilling for preparating the material, as well as Georg Oleschinski for the photographs of the juvenile specimens. Our gratitude also goes to Franziska Sumpf for 3D-modelling four of the specimens studied. All of the four are employed at the Steinmann Institute of the University of Bonn. Lastly we want to thank Armin Schmitt (Dinosaurierpark Münchehagen) for the discussions and ideas on the morphometric part of this study and Jessica Mitchell (Steinmann Institute of the University of

741 Bonn) for improving the English of the manuscript. This research was performed as MSc.
742 Thesis at the University of Bonn.
743

744 References

745 Allain R, Aquesbi N. 2008. Anatomy and phylogenetic relationships of *Tazoudasaurus naimi*
746 (Dinosauria, Sauropoda) from the late Early Jurassic of Morocco. *Geodiversitas* 30:345-424.
747
748 Barrett PM, Upchurch P. 2005. Sauropod diversity through time: possible macroevolutionary
749 and paleoecological implications. In: Curry-Rogers KA, and Wilson JA, eds. *Sauropod*
750 *Evolution and Paleobiology*. Berkeley: University of California Press, 125–156.

751 Bonaparte JF, Vince M. 1979. El hallazgo del primer nido de dinosaurios triásicos
752 (Saurischia, Prosauropoda). Triásico Suerior de Patagonia. Argentina. *Ameghiniana* 16:173-
753 182.

754 Bonaparte JF. 1999. Evolución de las vértebras presacras en Sauropodomorpha. *Ameghiniana*
755 36:115-187.

756 Brochu CA. 1996. Closure of neurocentral sutures during crocodilian ontogeny: implications
757 for maturity assessment in fossil archosaurs. *Journal of Vertebrate Paleontology* 16:49-62.
758
759 Carballido J, Marpmann J, Schwarz-Wings D, Pabst B. 2012. New information on a juvenile
760 sauropod specimen from the Morrison Formation and the reassessment of its systematic
761 position. *Palaeontology* 55:567-582.
762
763 Carballido JL, Sander PM. 2013. Postcranial axial skeleton of *Europasaurus holgeri*
764 (Dinosauria, Sauropoda) from the Upper Jurassic of Germany: implications for sauropod
765 ontogeny and phylogenetic relationships of basal Macronaria. *Journal of Systematic*
766 *Paleontology*. Available at doi:10.1080/14772019.2013.764935.
767
768 Carpenter K, McIntosh J. 1994. Upper Jurassic sauropod babies from the Morrison
769 Formation. In: Carpenter K, Hirsch KF, Horner JR, eds. *Dinosaur Eggs and Babies*.
770 Cambridge: Cambridge University Press, 265-278.
771
772 Carrano MT. 2006. Body-size evolution in the Dinosauria. In: Carrano MT, Blob RW,
773 Gaudin TJ, Wible JR, eds. *Amniote Paleobiology: Perspectives on the Evolution of Mammals,*
774 *Birds, and Reptiles*. Chicago: University of Chicago Press, 225-268.
775
776 Chinsamy A. 1993. Bone histology and growth trajectory of the prosauropod dinosaur
777 *Massospondylus carinatus* (Owen). *Modern Geology* 18:319-329.
778
779 Chinsamy-Turan A. 2005. *The microstructure of dinosaur bone*. Baltimore: Johns Hopkins
780 University Press.
781
782 Cooper MR. 1981. The prosauropod dinosaur *Massospondylus carinatus* Owen from
783 Zimbabwe: its biology, mode of life and phylogenetic significance. *Occasional Papers of the*
784 *National Museums and Monuments: Natural Sciences* 6(10):689-840.

785 Curry KA. 1999. Ontogenetic histology of *Apatosaurus* (Dinosauria: Sauropoda): New
786 insights on growth rates and longevity. *Journal of Vertebrate Paleontology* 19:654-665.
787
788 Curry KA, Erickson GM. 2005. Sauropod histology: microscopic views on the lives of giants.
789 In: Curry KA, Wilson JA, eds. *The Sauropods Evolution and Paleobiology*. Berkeley and Los
790 Angeles: University of California Press, 303-326.
791
792 Finckh A. 1912. Die Knollenmergel des Oberen Keupers. *Verein für vaterländische*
793 *Naturkunde in Württemberg* 68:29-32.

794 Foster JR. 2005. New juvenile sauropod material from western Colorado, and the record of
795 juvenile sauropods from the Upper Jurassic Morrison Formation. In: Tidwell V, Carpenter K,
796 eds. *Thunder–Lizards: The Sauropodomorph Dinosaurs*. Bloomington: Indiana University
797 Press, 141-153.
798
799 Fraas E. 1913. Die neuesten Dinosaurierfunde in der schwäbischen Trias.
800 *Naturwissenschaften* 45:1097-1100.
801
802 Gallina PA. 2011. Notes on the axial skeleton of the titanosaur *Bonitasaura salgadoi*
803 (Dinosauria-Sauropoda). *Anais da Academia Brasileira de Ciências* 83(1):235-245.
804
805 Galton PM. 1984a. An early prosauropod dinosaur from the upper Triassic of
806 Nordwürttemberg, West Germany. *Stuttgarter Beiträge zur Naturkunde*, Serie B, 106:1-25.
807
808 Galton PM. 1984b. Cranial anatomy of the prosauropod dinosaur *Plateosaurus* from the
809 Knollenmergel (Middle Keuper, Upper Triassic) of Germany. I. Two complete skulls from
810 Trossingen/Württemberg with comments on the diet. *Geologica et Palaeontologica* 18:139-
811 171.

812 Galton PM. 1985a. Cranial anatomy of the prosauropod dinosaur *Plateosaurus* from the
813 Knollenmergel (Middle Keuper, Upper Triassic) of Germany. II. All the cranial material and
814 details of soft-part anatomy. *Geologica et Palaeontologica* 19:119-159.
815
816 Galton PM. 1985b. Diet of prosauropod dinosaurs from the Late Triassic and Early
817 Jurassic. *Lethaia* 18:105-123.

818 Galton PM, Bakker RT. 1985. The cranial anatomy of the prosauropod dinosaur "*Efraasia*
819 *diagnostica*", a juvenile individual of *Sellosaurus gracilis* from the Upper Triassic of
820 Nordwürttemberg, West Germany. *Stuttgarter Beiträge zur Naturkunde*, Serie B, 117:1-15.

821 Galton PM. 1986. Prosauropod dinsosaur *Plateosaurus* (= *Gresslyosaurus)* (Saurischia:
822 Sauropodomorpha) from the Upper Triassic of Switzerland. *Geologica et Palaeontologica*
823 20:167-183.
824
825 Galton PM. 1997. Comments on sexual dimorphism in the prosauropod dinosaur
826 *Plateosaurus engelhardti* (Upper Triassic, Trossingen). *Neues Jahrbuch für Geologie und*
827 *Paläontologie, Monatshefte*, 1997:674-682.
828
829 Galton PM. 1999. Sex, sacra and *Sellosaurus gracilis* (Saurischia, Sauropodomorpha, Upper
830 Triassic, Germany) - or why the character "two sacral vertebrae" is plesiomorphic for
831 Dinosauria. *Neues Jahrbuch für Geologie und Paläontologie, Abhandlungen* 213:19-55.

PeerJ PrePrints | http://dx.doi.org/10.7287/peerj.preprints.325v1 | CC-BY 4.0 Open Access | received: 30 Mar 2014, published: 30 Mar 2014

Galton PM. 2000. The prosauropod dinosaur *Plateosaurus* MEYER, 1837 (Saurischia: Sauropodomorpha). I. The syntypes of *P. engelhardti MEYER*, 1837 (Upper Triassic, Germany), with notes on other European prosauropods with "distally straight" femora. *Neues Jahrbuch für Geologie und Paläntologie, Abhandlungen*, 216(2):233-275.

Galton PM. 2001. The prosauropod dinosaur *Plateosaurus* MEYER, 1837 (Saurischia: Sauropodomorpha; Upper Triassic), II. Notes on the referred species. *Revue de Paléobiologie, Genéve* 20:435-502.

Galton PM. 2012. Case 3560 *Plateosaurus engelhardti* Meyer, 1837 (Dinosauria, Sauropodomorpha): proposed replacement of unidentifiable name-bearing type by a neotype. *Bulletin of Zoological Nomenclature* 69(3):203-212.

Huene F von. 1926. Vollständige Osteologie eines Plateosauriden aus dem schwäbischen Keuper. *Abhandlungen zur Geologie und Palaeontologie 15*(2):1-43.

Huene F von. 1932. Die fossile Reptil-Ordnung Saurischia, ihre Entwicklung und Geschichte. *Monographie Geologie Paläontologie* Serie 1:1-361.

Ikejiri T. 2003. Sequence of closure of neurocentral sutures in *Camarasaurus* (Sauropoda) and implications for phylogeny in Reptilia. *Journal of Vertebrate Paleontology* 23(3 Supplement):65A.

Ikejiri T, Tidwell V, Trexler DL. 2005. New adult specimen of *Camarasaurus lentus* highlight ontogenetic variation within the species. In: Tidwell V, Carpenter K, eds. *Thunder-Lizards: The Sauropodomorph Dinosaurs*. Bloomington: Indiana University Press, 154-179.

Irmis RB. 2007. Axial skeleton ontogeny in the Parasuchia (Archosauria: Pseudosuchia) and its implications for ontogenetic determination in archosaurs. *Journal of Vertebrate Paleontology* 27(2):350-361.

Jaekel O. 1914a. Über die Wirbeltierfunde der oberen Trias von Halberstadt. *Paläontologische Zeitschrift*, 1:155-215.

Jenkins FA, Shubin NH, Jr., Amaral WW, Gatesy SM, Schaff CR, Clemmensen LB, Downs WR, Davidson AR, Bonde N, Osbaeck F. 1994. Late Triassic continental vertebrates and depositional environments of the Fleming Fjord Formation, Jameson Land, East Greenland. *Meddeleser om Grønland, Geoscience* 32:1-25.

Klein N, Sander PM. 2007. Bone histology and growth of the prosauropod *Plateosaurus engelhardti* MEYER, 1837 from the Norian bonebeds of Trossingen (Germany) and Frick (Switzerland). *Special Papers in Palaeontology* 77:169-206.

Klein N, Sander PM. 2008. Ontogenetic stages in the long bone histology of sauropod dinosaurs. *Paleobiology* 34:247-263.

Leal LA, Azevedo SAK, Kellner AWA, da Rosa AAS. 2004. A new early dinosaur (Sauropodomorpha) from the Caturrita Formation (Late Triassic), Paraná Basin, Brazil. *Zootaxa* 690:1-24.

Marpmann JS, Carballido J, Remes K, Sander PM. 2011. Ontogenetic changes in the skull elements of the Late Jurassic dwarf sauropod *Europasaurus holgeri*. *Journal of Vertebrate Paleontology*. 31(6):151A.

Martin V. 1994. Baby sauropods from the Sao Khua Formation (Lower Cretaceous) in Northeastern Thailand. *Gaia* 10:147-153.

Matter A, Peters T, Bläsi H-R, Meyer J, Ischi H, Meyer Ch. 1988. Sondierbohrung Weiach – Geologie (Textband). *Nagra Technischer Bericht NTB 86-01, Baden*: 470.

McIntosh JS. 1989. The sauropod dinosaurs: a brief survey. In: Padian K., Chure DJ, eds. *The Age of Dinosaurs*. Short courses in Paleontology number 2. Knoxville: University of Tennessee, 85-99.

Meyer H von. 1837. Mitteilungen, an Professor Bronn gerichtet (*Plateosaurus engelhardti*). *Neues Jahrbuch für Mineralogie, Geologie und Paläontologie*, 1837:817.

Moser M. 2003. *Plateosaurus engelhardti* Meyer, 1837 (Dinosauria: Sauropodomorpha) aus den Feuerletten (Mittelkeuper; Obertrias) von Bayern. *Zitteliana B*, 24:1-188.

Osborn HF. 1899. A skeleton of *Diplodocus*. *Memoirs of the American Museum of Natural History* 3:247-387.

Otero A, Pol D. 2013. Postcranial anatomy and phylogenetic relationships of *Mussaurus patagonicus* (Dinosauria, Sauropodomorpha). *Journal of Vertebrate Paleontology*, 33(5):1138-1168.

Reisz RR, Scott D, Sues H-D, Evans DC, Raath MA. 2005. Embryos of an early Jurassic prosauropod dinosaur and their evolutionary significance. *Science* 309:761-764.

Reisz RR, Evans DC, Roberts EM, Sues H-D, Yates AM. 2012. Oldest known dinosaurian nesting site and reproductive biology of the Early Jurassic sauropodomorph *Massospondylus*. *Proceedings of the National Academy of Sciene* 109:2428-2433.

Ricqlès A de, Padian KP, Horner JR. 2003. On the bone histology of some Triassic pseudosuchian archosaurs and related taxa. *Annales de Paléontologie* 89(2):67-101.

Rieber H. 1985. Der Plateosaurier von Frick. *Uni Zürich* 1985 (6):3-4.

Sander PM. 1990. Keuper und Lias der Tongrube Frick. In: Weidert WK, ed.: *Klassische Fundstellen*. Band II. Korb: Goldschneck Verlag, 89-96.

Sander PM. 1992. The Norian Plateosaurus bonebeds of central Europe and their taphonomy. *Palaeogeography, Palaeoclimatology, Palaeoecology* 93:255-299.

Sander PM. 1993. "Versumpft!" Die Fricker Plateosaurier. *Fossilien* 1993(5):303-309.

Sander PM. 1999. Life history of the Tendaguru sauropods as inferred from long bone histology. *Mitteilungen aus dem Museum für Naturkunde der Humboldt-Universitat zu Berlin*, Geowissenschaftliche Reihe 2:103-112.

PeerJ PrePrints | http://dx.doi.org/10.7287/peerj.preprints.325v1 | CC-BY 4.0 Open Access | received: 30 Mar 2014, published: 30 Mar 2014

928 Sander PM. 2000. Long bone histology of the Tendaguru sauropods: Implications for growth
929 and biology. *Paleobiology* 26:466-488.
930
931 Sander PM, Tückmantel C. 2003. Bone lamina thickness, bone apposition rates, and age
932 estimates in sauropod humeri and femora. *Paläontologische Zeitschrift* 76:161-172.
933
934 Sander PM, Klein N. 2005. Developmental plasticity in the life history of a prosauropod
935 dinosaur. *Science* 310:1800-1802.
936
937 Sander PM, Mateus O, Laven T, Knötschke N. 2006. Bone histology indicates insular
938 dwarfism in a new Late Jurassic sauropod dinosaur. *Nature* 441:739-741.
939
940 Sander PM, Klein N, Stein K, Wings O. 2011. Sauropod bone histology and its implications
941 for sauropod biology. In: Klein N, Remes K, Gee CT, Sander PM, eds. *Understanding the*
942 *Life of Giants: Biology of the Sauropod Dinosaurs: the evolution of gigantism*. Bloomington:
943 Indiana University Press, 276-302.
944
945 Sander PM. 2012. Der schwäbische Lindwurm: eine Detektivgeschichte. In: Martin T,
946 Koenigswald Wv, Radtke G, Rust J, eds. *Paläontologie – 100 Jahre Paläontologische*
947 *Gesellschaft*. München: Verlag Dr. Friedrich Pfeil, 108-109.
948
949 Seeley HG. 1870. On *Ornithopsis*, a gigantic animal of the pterodactyle kind from the
950 Wealden. *Annals and Magazine of Natural History* 4(5):279-283.
951
952 Sekiya T, Jin X, Zheng W, Shibata M, Azuma Y. 2013. A new juvenile specimen of
953 *Yunnanosaurus robustus* (Dinosauria: Sauropodomorpha) from Early to Middle Jurassic of
954 Chuxiong Autonomous Prefecture, Yunnan Province, China. *Historical Biology*. Available at
955 doi: 10.1080/08912963.2013.821702.
956
957 Taylor MP, Wedel MJ. 2013. Why sauropods had long necks; and why giraffes have short
958 necks. *PeerJ* 1:e36.
959
960 Tidwell V, Wilhite RD. 2005. Ontogenetic variation and isometric growth in the forelimb of
961 the Early Cretaceous sauropod *Venenosaurus*. In: Tidwell V, Carpenter K., (eds). *Thunder-*
962 *Lizards: The Sauropodomorph Dinosaurs*. Bloomington: Indiana University Press, 187-196.
963
964 Upchurch P, Barrett PM, Galton PM. 2007. A phylogenetic analysis of basal sauropodomorph
965 relationships: implications for the origin of sauropod dinosaurs. In: Barrett PM, Batten DJ,
966 eds. *Evolution and Palaeobiology of Early Sauropodomorph Dinosaurs*. *Special Papers in*
967 *Palaeontology* 77:57–90.
968
969 Weishampel DB. 1984. Trossingen: E. Fraas, F. von Huene, R. Seemann, and the
970 "Schwäbische Lindwurm" *Plateosaurus*. In: Reif WE, Westphal F, eds. *Third Symposium on*
971 *Terrestrial Ecosystems, Short Papers*. Tübingen: ATTEMPTO, 249-253.
972
973 Weishampel DB, Westphal F. 1986. Die Plateosaurier von Trossingen. *Ausstellungen und*
974 *Kataloge der Universität Tübingen*, 19:1-27.

975 Weishampel DB, Chapman RE. 1990. Morphometric study of *Plateosaurus* from Trossingen
976 (Baden-Württemberg, Federal Republic of Germany). In: Carpenter K, Currie PJ, eds.

977 *Dinosaur Systematics: Perspectives and Approaches*. Cambridge: Cambridge University
978 Press, 43-51.

979 Wilson JA. 1999. Vertebral laminae in sauropods and other saurischian dinosaurs. *Journal of*
980 *Vertebrate Paleontology* 19:639-653.
981
982 Wilson JA, D'Emic MD, Ikejiri T, Moacdieh EM, Whitlock JA. 2011. A nomenclature for
983 vertebral fossae in sauropods and other saurischian dinosaurs. *PLoS ONE* 6(2):1-19.
984
985 Yates AM. 2003. A new species of the primitive dinosaur *Thecodontosaurus* (Saurischia:
986 Sauropodomorpha) and its implications for the systematics of early dinosaurs. *Journal of*
987 *Systematic Paleontology* 1:1-42.

988
989
990
991
992
993
994
995
996
997
998
999
1000
1001
1002
1003
1004
1005

1006 *PeerJ PrePrints* | http://dx.doi.org/10.7287/peerj.preprints.325v1 | CC-BY 4.0 Open Access | received: 30 Mar 2014, published: 30 Mar 2014

Specimen Number	Position in vertebral column
MSF 11.3.317	Axis
MSF 11.3.258	C3
MSF 11.3.371	C4
MSF 11.3.074	C6
MSF 11.3.366	C10
MSF 11.3.388	C?
MSF 11.3.360	D3
MSF 11.3.376	D3
MSF 11.3.049	D4
MSF 11.3.067	D5
MSF 11.3.167	D5
MSF 11.3.095	D6
MSF 11.3.107	D6
MSF 11.3.339	D7
MSF 11.3.241	D10/D11
MSF 11.3.303	D10/D11
MSF 11.3.169	D?
MSF 11.3.348	Cd?
MSF 11.3.304	Cd?

Table 1: List of juvenile neural arches of bone field 11.3.

List of juvenile neural arches of bone field 11.3. with their respective position determined. The complete vertebral column of *Plateosaurus engelhardti* consists of 10 cervical vertebrae (Axis to C10) and 15 dorsal vertebrae (D1 to D15). Positions D3, D5, D6 and D10/D11 can be recognized twice in the sample size. Specimen MSF 11.3.348 is the only caudal vertebrae to be studied in the research since caudal neural arches at least in the posterior region do not reveal characters to make a determination of if its position impossible. Specimens MSF 11.3.388 and MSF 11.3.169 were not assignable to a position due to poor preservation.

Adult (osteological mature) specimens	Femur length (mm)
MSF 5B	565
MSF 23	610
SMNS 13200	685

Table 2: Femur lengths of the adult specimens MSF 5B, MSF 23 and SMNS 13200.

The femur length of the adult specimens MSF 5B, MSF 23 and SMNS 13200 with completely closed neurocentral sutures on their vertebral column. The femur length of specimen MSF 5B was calculated with the given scapula/femur ratio (76%) of specimen MSF 23 and the measured scapula length of MSF 5B, since the femur itself is not preserved.

PeerJ PrePrints | http://dx.doi.org/10.7287/peerj.preprints.325v1 | CC-BY 4.0 Open Access | received: 30 Mar 2014, published: 30 Mar 2014

Location	SMNS 13200 Zyg/Fe ratio (%)	MSF 11.3. Zygapophyses length (mm)	MSF 11.3. Femur length (mm)
C1			
C2 (axis)		77.4	
C3	21.4	117.7	549.2
C4	25.0	142.5	570.0
C5	25.1		
C6	22.1	129.7	586.3
C7	25.8		
C8	25.5		
C9	19.6		
C10	19.0	109.9	578.4
D1	17.8		
D2	16.5		
D3	16.1	77.1 (86.7)	478.9 (538.5)
D4	16.6	98.7	593.15
D5		94.2 (101.1)	
D6	19.7	108.5 (109.2)	550.5 (554.0)
D7	20.4	106.6	521.5
D8			
D9	17.8		
D10	20.4	110.8 (121.6)	542.1 (594.9)
D11	20.7		
D12	19.6		
D13	20.9		
D14	19.4		
D15			

Table 3: Calculated range of femur length of the MSF 11.3. specimens.

For the calculation of a range of femur length of the juvenile specimens MSF 11.3. specimens we only used the Zyg/Fe ratio of specimen SMNS 13200 due to completeness and good preservation of this specimen. The femur length of the juvenile specimens lies in between 479 and 595 mm. Lengths given in parentheses are again resulting from the longer specimen at positions occupied twice (refer to Table S1). The femur length estimate for the larger juvenile is between 539 mm and 595 mm and that for the smaller juvenile is between 479 mm and 593 mm.

PeerJ PrePrints | http://dx.doi.org/10.7287/peerj.preprints.325v1 | CC-BY 4.0 Open Access | received: 30 Mar 2014, published: 30 Mar 2014

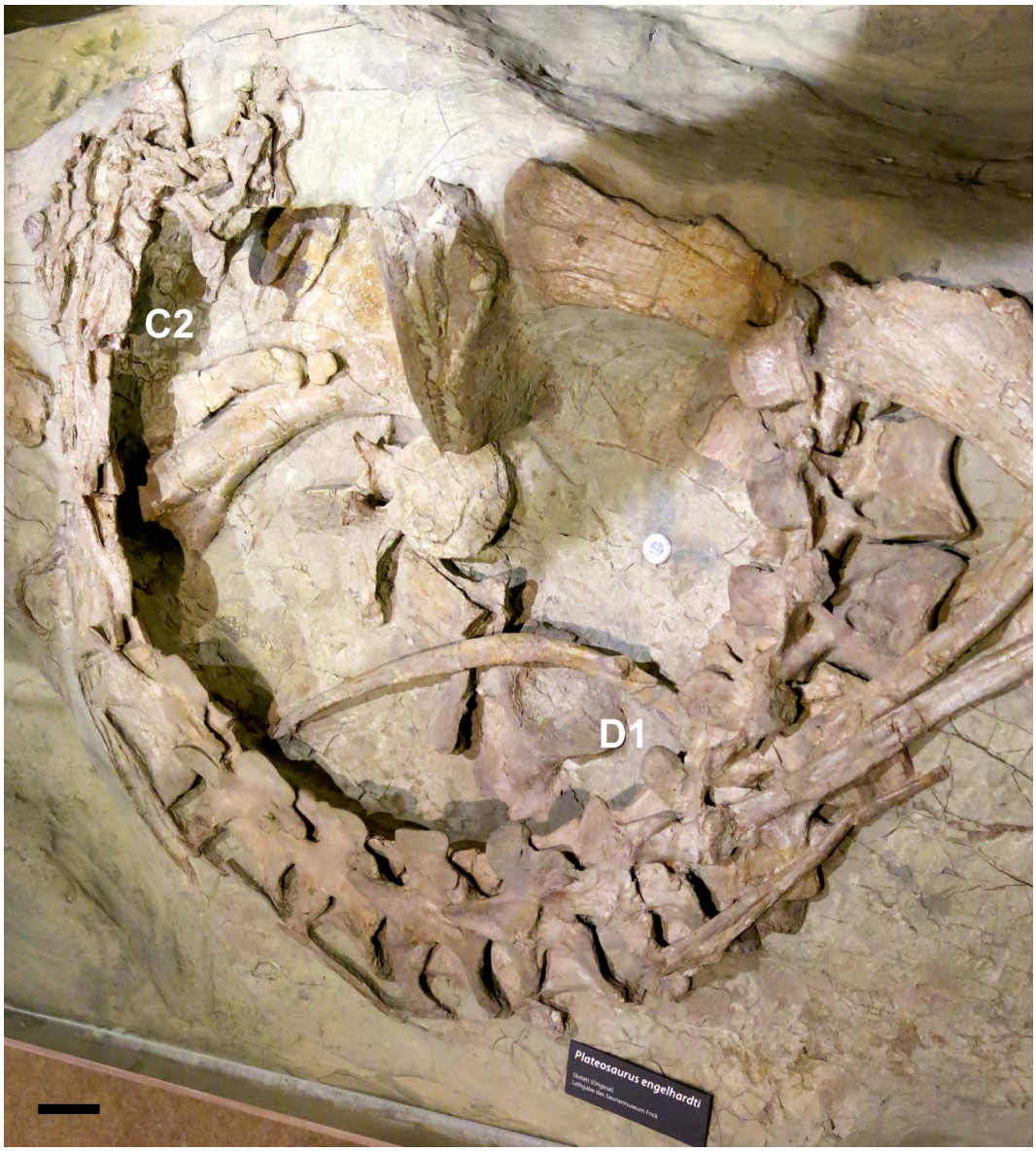

Figure 1: Specimen MSF 5 on exhibition in the SMA.

Specimen MSF 5B reveals a complete articulated cervical series from vertebrae C2 to C10 and articulated dorsal vertebrae from D1 to D5. MSF 5B. All zygapophyseal lengths were available for measurements. MSF 5B being an osteological mature specimen of *Plateosaurus engelhardti* shows completely closed neurocentral sutures with all morphological characters being well developed. Scale bar measures 5 cm.

Figure 2: Specimen MSF 23 on exhibition in the MSF.

Specimen MSF 23 is a nearly complete and in most parts articulated *P. engelhardti*. The cervical vertebrae series is complete from C1 to C10, but missing C7. The dorsal series is complete from D1 to D15. The vertebrae of this specimen are heavily deformed, especially in the posterior dorsal series making measurements difficult. This specimen shows completely closed neurocentral sutures and all morphological characters are well developed. Scale bar measures 20 cm.

PeerJ PrePrints | http://dx.doi.org/10.7287/peerj.preprints.325v1 | CC-BY 4.0 Open Access | received: 30 Mar 2014, published: 30 Mar 2014

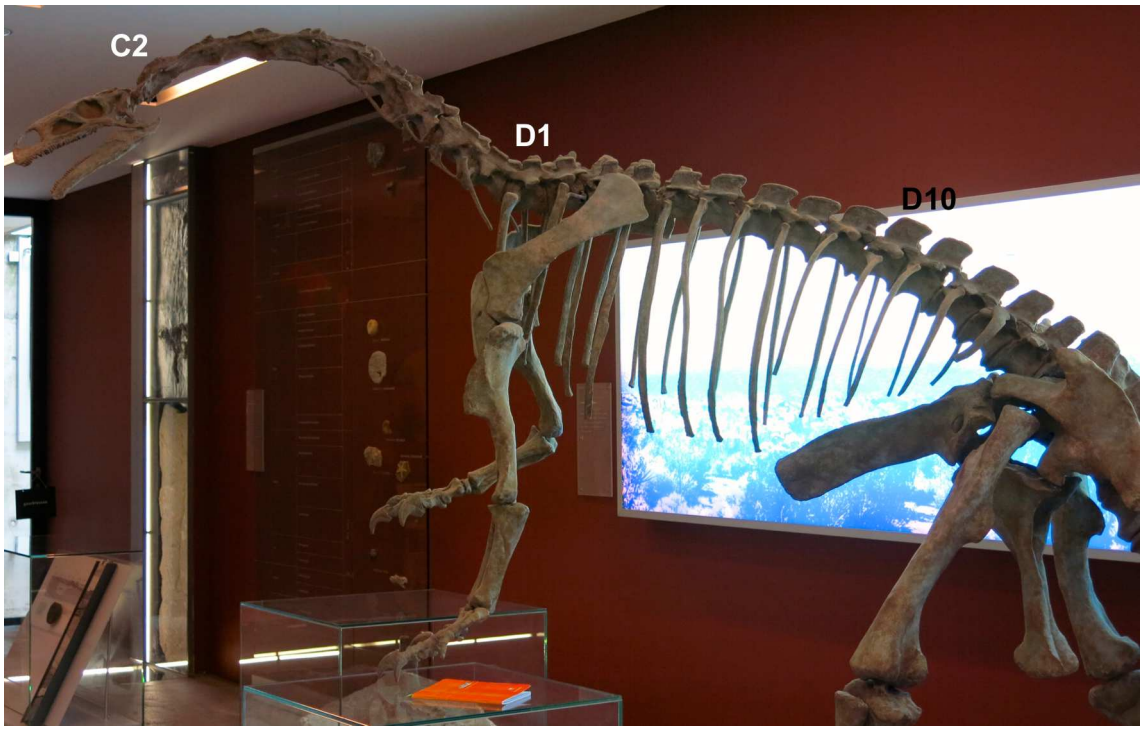

Figure 3: Specimen SMNS 13200: a cast exhibited in the NAA.

A complete mounted skeleton cast of SMNS 13200 from Trossingen, Germany. The cervical as well as the dorsal vertebrae series is well preserved. All neurocentral sutures are completely closed and all morphological characters are well developed. For scaling: the left femur length of specimen SMNS 13200 measures 68.5 cm.

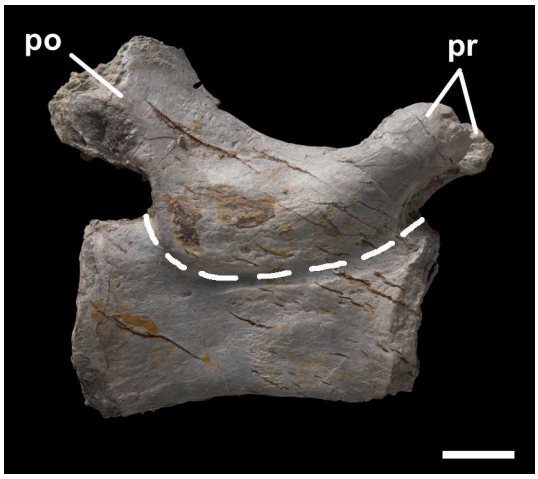

Figure 4: Caudal vertebrae MSF 11.3.348

MSF 11.3.348 is one of the caudal vertebrae in left lateral view found on bone field 11.3. The only morphological characters being present are the pre- and postzygapophyses. The neurocentral suture is completely closed as indicated by the line drawn. The whole caudal is interveined with dessication cracks. The scale bar measures 1 cm.

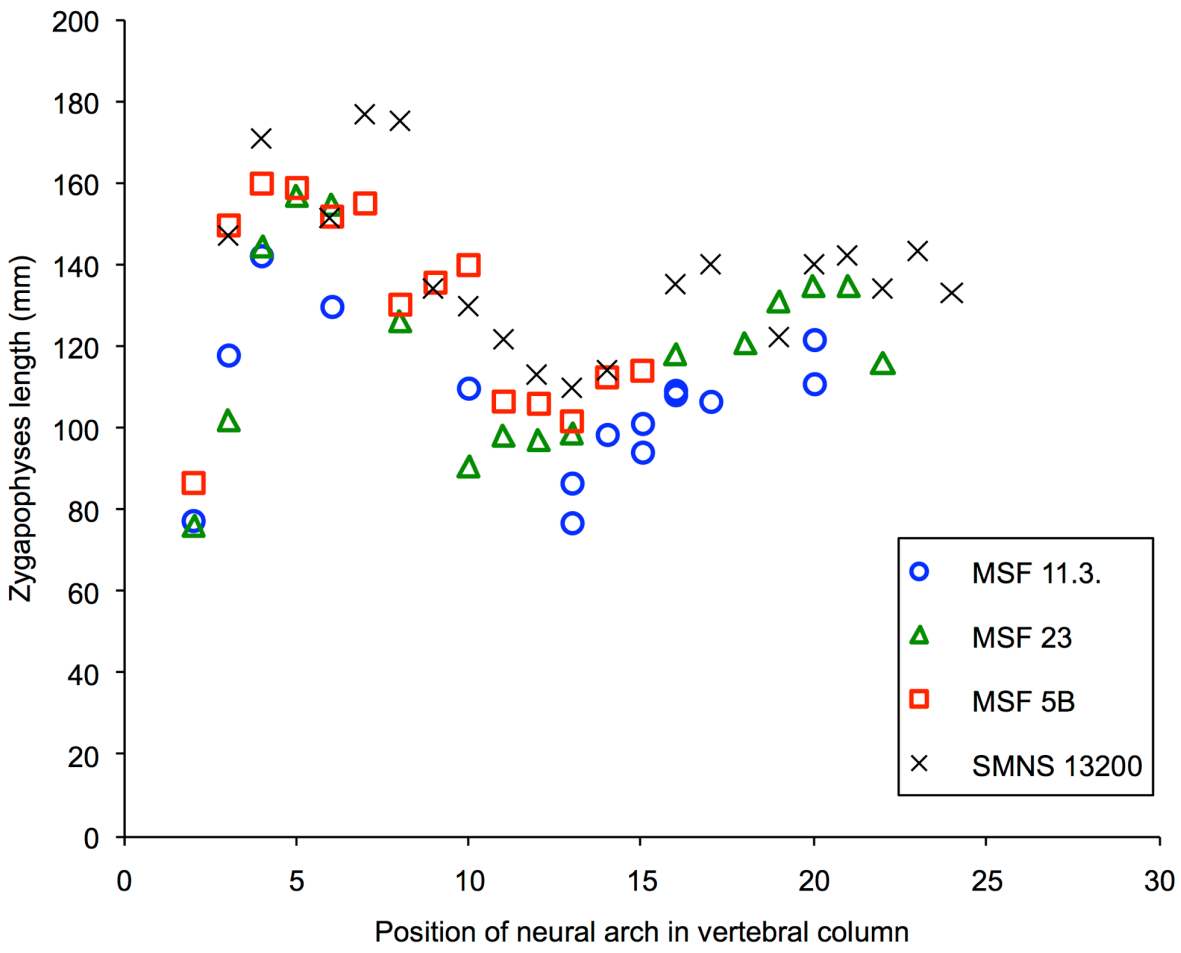

Figure 5: Zygapophyseal lengths in the vertebral column of specimen MSF 11.3., MSF 5B, MSF 23 and SMNS 13200.

The zygapophyseal lengths of all specimens follow a distinct pattern throughout the vertebral column. The zygapophyseal lengths show a sharp increase in the anterior cervical series. The posterior cervicals decrease in length reaching their minimum length at the third dorsal neural arch. Afterwards thex increase at a much lower rate than in the anterior cervical series. Specimen SMNS 13200 with the greatest femur length out of all specimens studied, also shows greater zygapophyseal lengths. The juvenile MSF 11.3. specimens generally show a zygapophyseal sitting below of those from the mature specimens and only intervene with those of MSF 23 at some positions in the posteriormost cervical series.

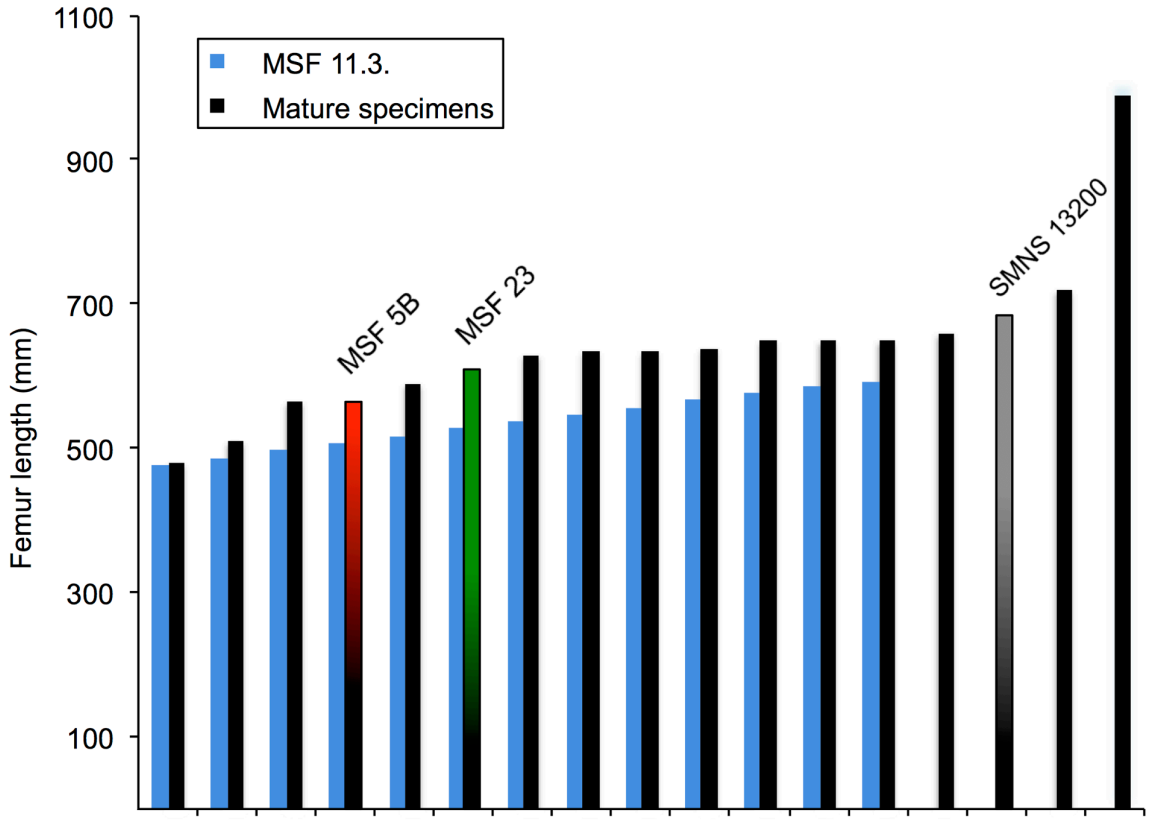

Figure 6: Size and maturity stage corrobating developmental plasticity

The femur lengths of the juvenile specimens of bone field 11.3. (blue) have been combined with the femur lengths of osteological mature specimens studied: MSF 5B (red/black), MSF 23 (green/black) and SMNS 13200 (gray/black); and the femur lengths of histological mature specimens (black) from Sander & Klein (2005). The femur length range of the juveniles has been divided up into 10 mm intervals to make it more practible in the diagram. The column diagram clearly shows the juvenile specimens and mature specimens merging into one another. The striking outlier of the whole diagram is specimen IFG with a remarkable great femur length of 990 mm. Nevertheless the diagram illustrates poor correlation between age (maturity) and size. Developmental plasticity is supported by histology as well as morphology.